ARTIFICIAL PHOTOSYNTHESIS, LIGHT DRIVEN ELECTRON TRANSFER PROCESSES
IN ORGANIZED MOLECULAR ASSEMBLIES AND COLLOIDAL SEMICONDUCTORS

Michael Grätzel

Institut de Chimie Physique, Ecole Polytechnique Fédérale,
CH-1015 Lausanne, Switzerland

Abstract – This article deals with artificial (non biological) systems that achieve
fuel generation by visible light. Intrinsic features of light driven redox processes
in organized assemblies such as surfactant micelles and colloidal semiconductors are
discussed. When coupled with suitable highly active redox catalysts these devices
can be employed to accomplish cleavage of water or hydrogen sulfide by visible light.

INTRODUCTION

Plant photosynthesis serves to convert light into energy-rich compounds such as carbohydrates.
This biological device is, however, a rather poor energy converter when the amount of biomass
produced by the incident solar flux is considered. Although the primary photoredox reactions
that occur in the chloroplasts proceed with high quantum efficiency the overall conversion
yield is approximately 5-6% and falls to < 3% at best when averaged over the whole year.
(Ref. 1)
Major losses are due to growth, adaptation and reproduction processes. Thus the photosynthe-
tic machinery could work more efficiently had it been designed mainly for fuel production
without any constraints due to evolutionary history. (Ref. 2)

Artificial systems try to overcome this shortcoming of the biological counterpart by simpli-
fying both the energy storing process and the molecular units that accomplish this transfor-
mation. Three different approaches are presently being persued. In the first or hybrid sys-
tem the thylakoid membranes or individual photosystems are employed as light harvesting units.
The objective is to exploit the high efficiency of the primary photosynthetic redox events
without attempting to synthesize carbohydrated from CO_2. Instead, hydrogen generation from
water is achieved through artificial redox relays and catalysts.

The second approach is to employ synthetic molecular assemblies such as micelles or membranes
as reaction systems. These aggregates simulate the microenvironment present in biological
systems and serve as a host for hydrophobic entities participating in the photoreactions.

Finally, artificial systems with very little resemblance to their biological counterpart are
also under study. Prominent and promising at the same time are here colloidal semiconductor
solutions.

Energy and electron transfer processes are of fundamental importance for all these energy
conversion devices. Thus, in photosynthesis antenna chlorophyll molecules perform the task
of light harvesting and light induced charge separation is achieved through vectorial elec-
tron transfer across the photosynthetic membrane. Similarly, the distinct microenvironment
present in molecular assemblies such as micelles and vesicles, in particular the presence of
a charged lipid/water interphase allows to kinetically control the charge transfer events.
Finally, in the case of small semiconductor particles it is the rapid movement of charge car-
riers in their respective band and the presence of local electrostatic fields at the particle/
water boundary which renders possible separation of oxidizing and reducing equivalents and
subsequent fuel formation from light.

A common feature of all these systems is their microheterogeneous character. As a consequence,
the electron transfer events occur within reaction spaces of minute dimension. This makes the
rate laws derived for homogeneous solutions inapplicable. New kinetic concepts had therefore
to be developed to interpret the experimental observations. These effects will be discussed
in the first section of this review dealing with intramicellar energy and electron transfer
processes. Subsequently photoinduced charge separation in functionalized surfactant assem-
blies will be discussed. The last part is dedicated to light excitation of colloidal semi-

conductors and the combination of the photoreaction with catalytic events leading to cleavage
of water and hydrogensulfide.

INTRAMICELLAR ELECTRON TRANSFER

Photoinduced electron transfer in simple surfactant micelles
In 1975 we carried out the first experiment on light induced electron transfer reactions in
micellar assemblies. (Ref. 3) Phenothiazine (PTH) was incorporated into sodium lauryl sul-
fate micelles and served as the photoactive electron donor while Eu^{3+} ions present at the
Stern layer of the aggregates were the electron acceptor, Fig. 1.

INTERFACIAL ELECTRON TRANSFER IN MICELLAR ASSEMBLIES
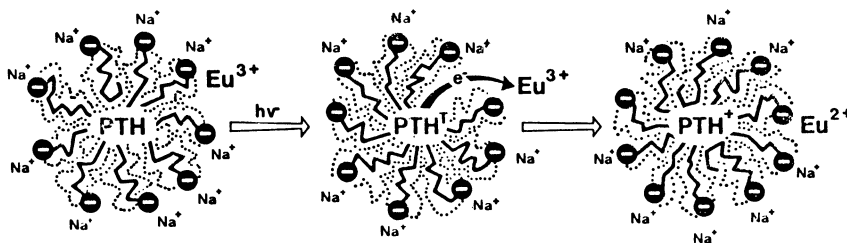
Fig. 1. First investigation of intramicellar electron transfer induced by
light. (Ref. 3) Triplet state phenothiazine was used as a donor and euro-
pium (III) ions as acceptor.

The dynamics of the reaction

$$PTH(T) \ + \ Eu^{3+} \ \longrightarrow \ PTH^+ \ + \ Eu^{2+} \tag{1}$$

where PTH(T) represents the triplet state of phenothiazine, were investigated by laser photo-
lysis technique. The decay was completed within a few hundred nanoseconds and could not be
fitted to a simple rate law. It was soon recognized that the rate laws previously derived
for intramicellar quenching processes (Ref. 4) were also applicable to electron transfer
reactions. The first case analyzed in detail in this manner was the photoinduced reduction
of $Ru(bipy)_3^{2+}$ by N-methyl phenothiazine (MPTH) (Ref. 5)

$$*Ru(bipy)_3^{2+} \ + \ MPTH \ \longrightarrow \ Ru(bipy)_3^{1+} \ + \ MPTH^+ \tag{2}$$
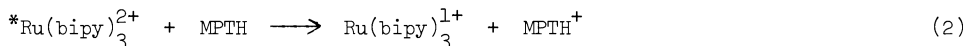
where $*Ru(bipy)_3^{2+}$ designates the charge transfer excited state of the ruthenium complex.
The temporal behaviour of this excited state after laser excitation is described by

$$[*Ru(bipy)_3^{2+}] \ = \ [*Ru(bipy)_3^{2+}](o) \ exp\{-k_d \ t + \bar{n}_A[exp(-k_q \ t)-1]\} \tag{3}$$

where $\bar{n}_A$ is the average number of MPTH molecules per micelle and k_d designates the specific
rate of excited state deactivation in the absence of MPTH. The parameter k_q has the dimen-
sion s^{-1} and corresponds to the rate of electron transfer in micelles containing only one
pair of reactands   The kinetic evaluation carried out for tetradecyltrioxyethylene sulfate
(TTOES) micelles yields for the specific rate of electron transfer between one donor acceptor
pair a value of $k=(6\pm0.3)x10^6 s^{-1}$ implying that the average time required for electron trans-
fer between a donor/acceptor pair associated with a host micelle is ca 160ns. A similar
value was obtained for the average time of intramicellar collisional triplet energy transfer
between a pair of reactants (Ref. 6).

Apparently, in order for the electron transfer event to occur close encounter of the reac-
tants is required. This rules out, at least for room temperature conditions, any signifi-
cant contribution of long range electron tunnelling to the overall rate of the electron
transfer process and confirms that light induced redox reactions in micellar aggregates occur
mainly via diffusional encounter of the reactants. The salient kinetic features of photo-
initiated intramicellar electron transfer reactions evolving from these investigations may be
summarized as follows: (i) the excited state decay is described by a multiexponential time
law; (ii) Stern-Volmer kinetics are not obeyed; (iii) if the products of the redox reaction

$$D \ + \ A \ \underset{}{\overset{h\nu}{\rightleftharpoons}} \ D^+ \ + \ A^- \tag{4}$$

i.e. D^+, A^- remain associated with their host aggregate electron back transfer between the
$D^+ \ ... \ A^-$ pair will occur. This reaction follows also first order kinetics and has the same
rate constant, i.e. $10^7 s^{-1}$, as that of the forward electron transfer; (iv) both forward and

backward electron transfer occur mainly through diffusional encounter of the reactants and long range tunnelling does not play a dominant role.

It should be noted that these findings contrast sharply with the kinetic picture for conventional homogeneous solution systems. One benefit of using compartmented systems such as micelles is that the reactants are brought in close proximity which enhances significantly the rate of the electron transfer event. Another advantage is that the local electrostatic potential of the micellar double layer can be exploited to achieve light induced charge separation, i.e. inhibit the thermal back electron transfer. Consider, for example, a situation where the electron donor is tetrathiafulvalene (TTF) and the acceptor is the anionic porphyrine (Ref. 6) $ZnTPPS^{4-}$, Fig. 2.

LIGHT INDUCED CHARGE SEPARATION IN MICELLAR ASSEMBLIES
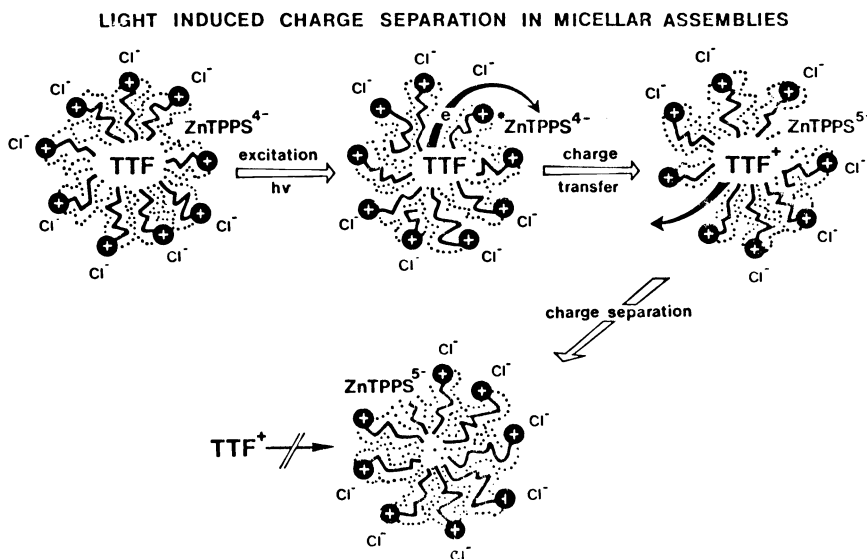
Fig. 2. The TTF/porphyrin system as an example for light induced charge separation by ionic micellar assemblies. (Ref. 6)

The porphyrin is excited by visible light which promotes electron transfer from TTF to $ZnTPPS^{4-}$. The radical ion pair $TTF^+/ZnTPPS^{5-}$ is thereby produced within the aggregate. In a cationic micelle TTF^+ is clearly distabilized with respect to the aqueous bulk solution. Therefore, once it reaches the surface it will be ejected into the water. Conversely, the $ZnTPPS^{5-}$ radical is electrostatically more stable in the micellar than in the aqueous phase and will thus remain associated with the surfactant aggregate. Once A^- and D^+ are separated their diffusional re-encounter is obstructed by the ultrathin barrier of the micellar double layer. Figure 3 illustrates the successful charge separation in the $ZnTPPS^{4-}/TTF$ system by cationic hexadecyltrimethylammoniumchloride micelles (CTAC).
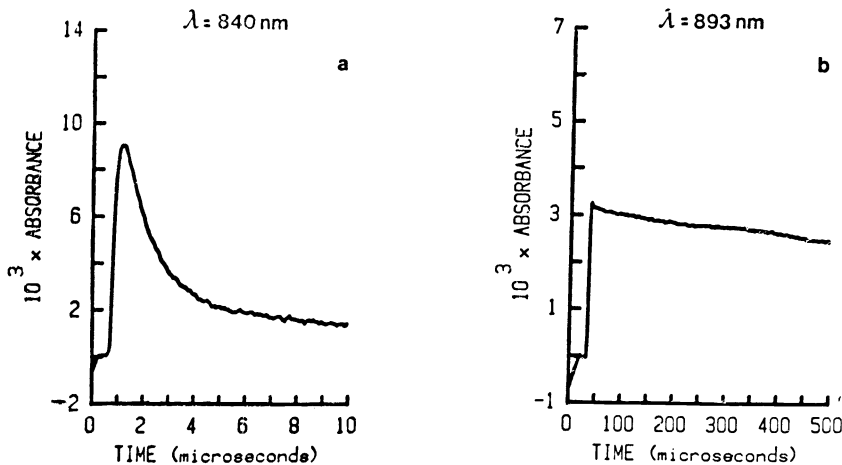
Fig. 3. Absorption decay curves of $ZnTPPS^{4-}$ triplet ($\lambda=840$nm) and $ZnTPPS^{5-}$ anion radicals ($\lambda=893$nm) in CTAC micellar solution. [CTAC] = 2.5×10^{-3}M; [TTF] = 2.5×10^{-3}M; [$ZnTPPS^{4-}$] = 4×10^{-5}M.

The porphyrine was excited by a 530nm laser pulse and the decay of the triplet state and formation of ZnTPPS^{5-} monitored at 840 and 893nm, respectively. (Ref. 6) The forward reaction follows the multiexponential time law given by eq 3 and from the kinetic analysis one obtains $k_q = 7x10^4 s^{-1}$. Through subsequent ejection of TTF$^+$ from the CTAC micelles the back reaction is impaired, the decay of ZnTPPS^{5-} being hardly visible on a 500µs timescale. In striking contrast to these results one finds in homogeneous solutions, e.g. methanol, no formation of redox products from the reductive quenching of triplet ZnTPPS^{4-} by TTF. Practically all radical ions (TTF$^+$/ZnTPPS^{5-}) apparently undergo back reaction in the solvent cage. This system provides an illustrative example how, by using molecular assemblies light induced charge separation can be achieved. In general the efficiency of the charge separation process will crucially depend on the relative rates of ejection and intramicellar back transfer of electrons from A$^-$ to D$^+$. The latter reaction is thermodynamically favorable and can in principle occur very rapidly. The rate of ejection of an ion from a charged micelle on the other hand is expected to depend critically on the degree of hydrophobic interaction of A$^-$ with the aggregated surfactant molecules.

Using this principle, light induced charge separation has been achieved for a number of donor/acceptor pairs. Noteworthy are the examples where pyrene served as an electron acceptor and dimethyl aniline as a donor (Ref. 7,8) as well as the photoinduced reduction of duroquinone by chlorophyll-a. (Ref. 9) The laser photolysis analysis of the latter system showed that a large fraction of Chla$^+$ does not undergo back reaction with the reduced quinone (DQ$^-$) due to efficient ejection of the latter from the micellar into the aqueous phase. The rate of DQ$^-$ ejection was estimated to be $10^{-8} s^{-1}$. Since the intramicellar back reaction occurs typically at 10-20 times smaller rate one infers that the DQ$^-$ escape yield from the micelle is at least 80%. As the reentry of DQ$^-$ into the surfactant assembly is prevented by the micellar surface charge, the lifetime of Chla$^+$ is prolonged by several orders of magnitude with respect to homogeneous solutions.

Light initiated redox reactions in functional micelles
Further progress in the development of molecular assemblies capable of converting light energy into chemical energy was made by designing and synthesizing surfactants with suitable functionality. These are distinguished from simple surfactants by the fact that the micelle itself participates in the redox events. Figure 4 juxtaposes a conventional anionic surfactant aggregate to a functional one where the counter ion atmosphere is constituted by a transition metal ion, such as Cu^{2+} or Eu^{3+} which is reduced by the excited state of a solubilized sensitizer. The role of the conventional micelle in a photoredox reaction, as described in the previous section, was to provide solubilization sites for hydrophobic reactants and to assist in light induced charge separation. Functionalized micelles have the additional advantage of displaying cooperative effects which will be illustrated in the examples below.

SIMPLE MICELLE :

Provides hydrophobic sites for reaction and local potential for charge separation e.g. surfactant : sodiumlauryl sulfate.

$$CH_3-(CH_2-)_{11} OSO_3^- Na^+$$
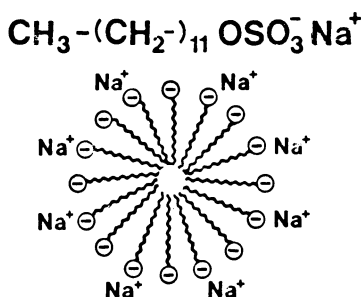
FUNCTIONAL MICELLE :

Participates in redox reaction. Functionalized counter ion

$$D + M^{n+} \xrightleftharpoons[\Delta]{h\nu} D^+ + M^{(n-1)+}$$
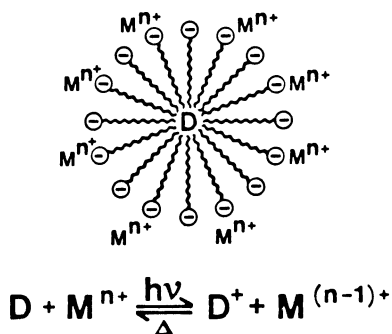
Fig. 4. Intervention of simple and functionalized micelles in photoredox reactions.

Consider first the case of a transition metal ion micelle which can be obtained, for example, by replacing the Na$^+$ ions in sodium lauryl oxyethylene sulfate by cupric ions. (Ref. 10, 11) The electron transfer occurs here from a solubilized sensitizer to the counter ion atmosphere. An illustrative example is that where D=N,N'-dimethyl-5,11-dihydroindolo 3,3-6 carbazole (DI). When dissolved in NaLS micelles, DI displays an intense fluorescence and the fluorescence lifetime measured by laser techniques is 144ns. Introduction of Cu^{2+} as counter ion atmos-

phere induces a 30 fold decrease in the fluorescence yield and lifetime of DI. The detailed laser analysis of this system showed that in Cu(LS) micelles there is an extremely rapid electron transfer from the excited singlet to the Cu^{2+} ions. This process occurs with an average time of 4ns and hence can compete efficiently with fluorescence and intersystem crossing. This astonishing result must be attributed to a pronounced micellar enhancement of the rate of the transfer reaction. It is, of course, a consequence of the fact that within such a functional surfactant unit, regions with extremely high local concentrations of Cu^{2+} prevail. (Theoretical estimates predict the counter ion concentration in the micellar Stem layer to be between 3 and 6 M). The previously developed theoretical approach for intramicellar redox reactions (Ref. 12) can explain satisfactorily such a behavior. In fact, the case where an excited species, S^*, distributed initially in a random fashion within a surfactant assembly, diffuses to a reactive interface can be treated mathematically in a closed fashion. Ficks equation

$$\frac{\partial [S^*]\,(r,t)}{\partial t} \;=\; D\nabla^2 [S^*]\,(r,t) \tag{5}$$

has to be solved subject to the following three boundary conditions

$$[S^*]\,(r_o,t) \;=\; 0 \qquad \text{all } t \tag{6}$$

$$[S^*]\,(r,o) \;=\; [S^*]_o \qquad \text{all } r < r_o \tag{7}$$

$$\lim r \cdot [S^*]\,(r,t) \longrightarrow 0 \quad \text{all } t \tag{8}$$

In eq (5) $[S^*]\,(r,t)$ is the (ensemble averaged) concentration of the excited sensitizer inside the micelle at time t and at a distance r from the center of the micelle, D is the diffusion coefficient, and ∇^2 the Laplacian operator. The micellar radius is represented by r_o. The boundary condition (6) expresses the fact that the surface of the micelle is instituted by reactive transition metal ions and hence may be regarded as a perfectly absorbing boundary for S^*. The second condition (7) specifies that at time t=0, all interior positions of the micelle are accessible to the confined, diffusing species, i.e. no localization of the confined species is assumed at t=0. The limit specified by eq (8) is a finiteness condition which formalizes the physical constraint that the reactant concentration remains finite for all times and all interior points of the assembly. The integration of eq (5) gives first the concentration of sensitizer as a function of both radical position and time. After spatial averaging one obtains for the experimentally measured quantity

$$[S^*]\,(t) \;=\; \frac{6[S^*]_o}{\pi^2} \sum_{n=1}^{\infty} \frac{1}{n^2} \exp\frac{-n^2\pi^2 D}{r_o^2}\,t \tag{9}$$

Given the exponential structure of this equation, on a time scale for which $t > r_o^2/\pi^2 D$, the n=1 term in the summation will dominate the kinetic behavior of the system. Since the ratio $r_o^2/\pi^2 D$ for micellar aggregates is typically of the order of a few ns, a necessary consequence of eq (9) is that kinetic processes which take place on a time scale greater than a ns should exhibit essentially first order kinetics. This is indeed observed in the case of the luminescence decay of DI in the Cu^{2+} counter ion micelles described above. From eq (9) a fluorescence lifetime of 4ns, i.e. a rate constant for electron transfer from DI* to Cu^{2+} of $2.5\times10^8 s^{-1}$, is compatible with a micellar radius of 15Å and a diffusion coefficient of $5\times10^{-7} cm^2/s$. It is important to note that the rate constant observed in this functionalized micelle is about 50 times greater than that for electron transfer between a donor acceptor pair in a simple surfactant aggregate.

The significance of this functional organization becomes evident also when the back reaction of Cu^+ and DI^+ is considered. Previous studies have shown that the intramicellar electron transfer from Cu^+, to DI^+, though thermodynamically highly favorable, cannot compete kinetically with the escape of the cuprous ion from its native micelle into the aqueous phase. An efficient escape route is provided by the exchange with one of the Cu^{2+} ions present in high local concentration in the Guoy-Chapman layer. By mere electrostatic arguments the latter ion is $\exp(e\Psi/kT)$ times more likely to be absorbed on the micellar surface than Cu^+. Once in the aqueous phase Cu^+ can be used for a second redox process such as the reduction of $Fe(CN)_6^{3-}$. The back reaction of the $Fe(CN)_6^{4-}$ with the oxidized donor, DI^+, is prevented by the negatively charge micellar surface. Hence, such a system is successful in storing light energy originally converted into chemical energy during the photoredox process.

Over the last years more sophisticated functionalized surfactants have been developed that show unique and highly promising effects in light induced charge separation. Thus, crown ether type amphiphiles complexed with suitable transition metal ions have been successfully employed as molecular electron storage devices. (Ref. 13) Similarly, surfactant derivatives of phenothiazine, when aggregated to micellar assemblies undergo monophotonic photoionization (Ref. 14) and afford storage of positive charges (holes). Finally, using amphiphilic viologen derivatives a new type of charge separation process has recently been developed. (Ref. 15) These phenomena have already been dealt with in earlier reviews (Ref. 16) and hence will not be adressed here in more detail.

INTERFACIAL ELECTRON AND HOLE TRANSFER REACTIONS IN COLLOIDAL SEMICONDUCTOR DISPERSIONS

In the following section we shall be concerned with interfacial electron transfer processes in yet another type of colloidal light harvesting device, i.e. semiconductor dispersions of extremely small particle size. In view of the importance of these devices for the utilization of solar energy, it is highly desirable to obtain detailed experimental information on the dynamics of photoinduced conduction or valence band processes involving species in solution. In the case of solid semiconductor electrodes a direct study of the kinetics of these reactions is made exceedingly difficult by the response of the electrical circuit to phenomena unrelated to the electron transfer event at the interphase. Similarly, the study of macro-dispersions of semiconductor powders is hampered by the high turbidity of these systems, rendering impossible the observation of transient species by fast kinetic spectroscopy.

In connection with our program on the light induced cleavage of water into hydrogen and oxygen, we became intrigued with the idea of investigating monodisperse semiconducting particles of small enough dimension to render scattering of light negligibly small. These have the advantage of yielding clear dispersions allowing for ready kinetic analysis of interfacial charge transfer processes by laser photolysis technique. The method consists in exciting the colloidal semiconductor particle directly by a very short flash of band gap irradiation. The subsequent reaction of conduction band electrons and valence band holes with reactants in solution is followed using fast kinetic spectroscopy or conductometry. The competitive trapping of electrons by noble metal catalysts, deposited onto the semiconductor particle to mediate hydrogen generation from water, can also be investigated. Finally, this study establishes a technique to determine the flat band potential of ultrafine colloidal semiconductors.

Basic kinetic considerations

We shall first consider the question of light absorption by these ultrafine particles. The maximum absorption coefficients for the semiconductor materials investigated is of the order of $10^5 cm^{-1}$ corresponding to an absorption length of at least 1000Å. In view of their small dimension (50 to 100Å), light traverses many particles before complete extinction has occurred, thus producing electron-hole pairs spatially throughout the particles along the optical path. This distinguishes the colloidal particles from semiconductor powders or electrodes where charge carriers are created mainly near the surface.

Consider a situation where a colloidal semiconductor particle such a TiO_2 is excited by a short (∼10ns) laser pulse resulting in the generation of electron-hole pairs, Fig. 5. The reaction of the conduction band electrons with a relay compound R present in the bulk solution is observed subsequently by kinetic spectroscopy. The hole is trapped readily by surface hydroxyl groups leading to water oxidation; the back charge-transfer into the particle is thus assumed to be negligible. In the specific case to be discussed, methyl viologen is used as an electron relay. The overall process of reduction of MV^{2+} by conduction-band electrons is described by three elementary steps, Fig. 6.
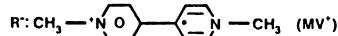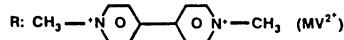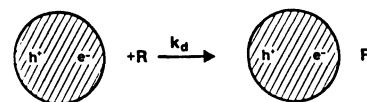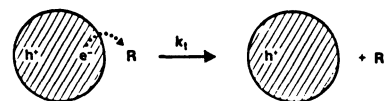
Fig. 5. Laser excitation of a colloidal semiconductor particle by a short pulse of band gap radiation and subsequent electron transfer to a relay compound R.

Fig. 6. Elementary processes involved in the charge transfer from the semiconductor particle to the relay compound, i) diffusion of charge carriers to to the particle surface, ii) encounter-complex formation with relay compound, iii) interfacial electron transfer.

i) <u>Diffusion of charge carriers from the particle interior to the interphase</u>. It is of interest to calculate the average transit time for a charge carrier from the interior to the surface of the colloidal semiconductor. For this purpose we can directly employ eq (9) which defines the time law of migration of a reactive species from the interior to the surface of a spherical aggregate of radius r_0. Thus one obtains for the average transit time

$$\tau = \frac{r_0^2}{\pi^2 D} \tag{10}$$

where D is the diffusion coefficient for electrons (or holes) in the semiconducting particle. D is related to the carrier mobility via

$$D = \mu \frac{k \cdot T}{e} \tag{11}$$

For TiO_2 particles with r_0=100Å and an electron mobility of $0.5cm^2/Vs$ one calculates τ=10ps. This transit time is much faster than the estimated value of 100ns for recombination, calculated for bulk recombination in a direct-band-gap semiconductor with a majority carrier density of $10^{17}cm^{-3}$. A similar estimation (Ref. 17) yields a recombination time of 100ps at a majority carrier density of $2 \times 10^{19}cm^{-3}$. Note that τ increases with the square of the particle radius. In the case of TiO_2 powders, a typical particle size would be 1μ which corresponds to τ=100ns.

These examples illustrate very clearly the distinct advantages of employing semiconductor particles of colloidal dimensions as photon harvesting units in solar energy conversion devices. Scattering effects are reduced to a minumum and the transit time of charge carriers from the interior to the particle surface is so short that electron-hole recombination cannot compete to any significant extent. Hence provided that electrons or holes are scavenged efficiently at the semiconductor-water interphase in comparison with surface recombination, photodriven chemical processes can be performed with a very high yield. It is noteworthy that for very small particles, an internal electrostatic field is not necessary to separate the photogenerated electron-hole pair.

ii) <u>Encounter-complex formation with the electron (or hole) acceptor present in solution</u>. In order that electron transfer can occur, an encounter complex must first be formed between the semiconductor particle and the electron relay present in the bulk solution. The rate of this process is diffusion limited and hence determined by the viscosity of the medium and the radius of the reactants. Not that this diffusional displacement will play no role in systems where the relay adheres to the particle surface.

iii) <u>Interfacial electron transfer</u>. This is a heterogeneous process which involves the movement of an electron from the conduction band of the semiconductor particle across the Helmholtz layer to the acceptor molecule. The rate constant of this process (k_{et}) is expressed consequently in units of cm/s. -

The sequence of encounter-complex formation between the semiconductor particle and relay and subsequent electron transfer can be treated kinetically by solving Ficks second law of diffusion. One obtains for the observed bi-molecular rate constant for electron transfer the expression

$$\frac{1}{k_{obs}} = \frac{1}{4\pi r^2} \left(\frac{1}{k_{et}} + \frac{r}{D} \right) \tag{12}$$

where r is the reaction radius corresponding to the sum of the radii of semiconductor particle and electron relay and D is the sum of their respective diffusion coefficients. The structure of eq (12) suggests two limiting cases:

1) $k_{et} >> \frac{D}{r}$, in this case the reaction is mass-transfer limited and eq (12) reduces to the familiar Smoluchowski expression:

$$k_{obs} = 4\pi r D \tag{13}$$

This condition means that for semiconductor particles with a radius of 100Å and a relay with a diffusion coefficient of ca. $10^{-5}cm^2/s$, k_{et} will only be sufficiently large if greater than 10cm/s. This is a high electrochemical rate constant and many redox couples will require substantial overvoltage to reach values as high as this.

2) $k_{et} >> \frac{D}{r}$. Here the heterogeneous electron transfer at the particle surface is rate limiting and eq (12) simplifies to

$$k_{obs} = 4\pi r^2 \cdot k_{et} \tag{14}$$

As k_{et} depends on the potential of the semiconductor particle one would expect that under these conditions, k_{obs} would also be a function of the overvoltage available to drive the interfacial electron-transfer event.

Dynamics of methyl viologen reduction by conduction band electrons of colloidal TiO₂ particles, flatband potential of colloidal TiO₂

These considerations will now be applied to analyze the dynamics of electron transfer from colloidal TiO₂ to methyl viologene (MV^{2+}). The latter is known to undergo a reversible one electron reduction with a well defined and pH independent redox potential (E^o = -440 mV against NHE). Furthermore, the reduced form (MV^+) can be readily identified by its characteristic blue color corresponding to an absorption maximum of 602nm (ε=11000 $M^{-1}cm^{-1}$).

Upon exposure of a deaerated TiO₂ sol to near-UV light in the presence of MV^{2+} the formation of this blue colored species becomes readily apparent. Both the growth kinetics of MV^+ as well as its yield were found to be strongly pH dependent. (Ref. 19) In Fig. 7 is illustrated the effect of pH on the yield of MV^+ after completion of the electron transfer.
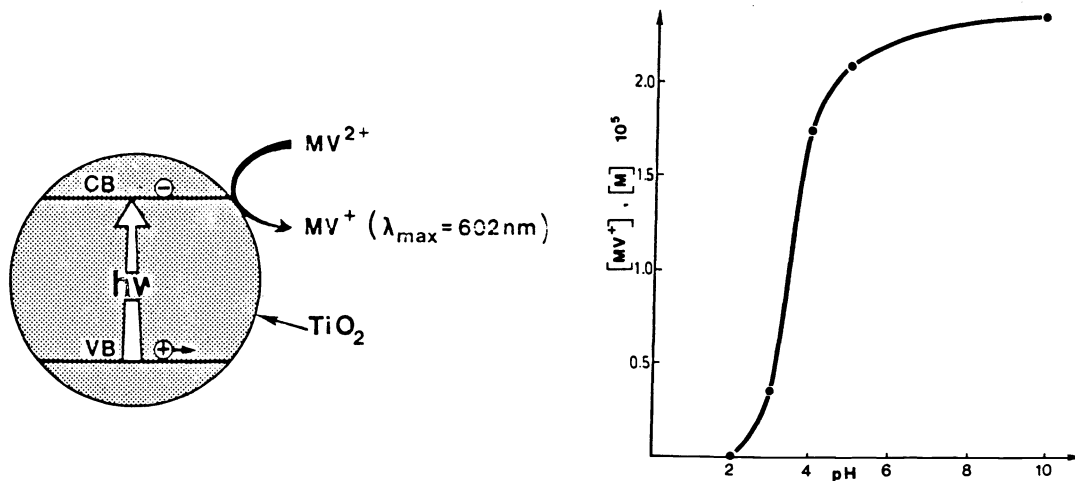
Fig. 7. Effect of pH on the yield of MV^+ after completion of interfacial electron transfer from colloidal TiO₂ [TiO₂] = 500mg/1, $[MV^{2+}]$ = 10^{-3}M.

(In these experiments, the colloidal TiO₂ particles (500mg/1) were excited with a 347.1 nm ruby laser flash and the MV^{2+} concentration was invariably 10^{-3}M.) This curve exhibits a sigmaoidal shape: No reduction of MV^{2+} occurs at pH≤2. The yield of MV^+ increases steeply between pH 2.5 and 5 and attains a plateau for neutral and basic solutions where $[MV^+]$ = $2.5x10^{-5}$M.

The results depicted in Fig. 7 can be used to derive the flat band potential (E_{fb}) of the colloidal TiO₂ particles. The reasoning is as follows: Due to an intrinsic oxygen deficiency, TiO₂ is an n-type semiconductor with the Fermi level (E_f) more or less close to the conduction band (E_{CB}). Laser excitation of TiO₂ leads to nonequilibrium population in e_{CB}^- and h^+ and therefore splitting of E_f into two quasi Fermi levels: one for the hole and one for the electron, $E_f(e^-)$. The latter merges practically with the conduction band as the carrier density produced by the laser flash in the TiO₂ particles exceeds $10^{19}cm^{-3}$. In the presence of MV^{2+} $E_f(e^-)$ will equilibrate with the Fermi level of the redox couple in solution

or
$$E_f(e^-) \quad = \quad E_f(MV^{2+}/MV^+) \tag{15}$$

$$E_f(e^-, \text{pH } 0)-0.059 \times \text{pH} \quad = \quad E^o(MV^{2+}/MV^+) + 0.059 \log \frac{MV^{2+}}{MV^+} \tag{16}$$

where $E^o(MV^{2+}/MV^+)$ = -0.445 V (vs. NHE). If equilibration takes place at relatively low pH only few acceptor ions will be converted to the reduced state. Thus the fraction of electrons that leave the particle is small so that the condition $E_f(e^-) = E_{CB}$ is still valid. Applying eq (16) to the data in Fig. 7 below pH 3.5, i.e. plotting log $([MV^+]/[MV^{2+}])$ against pH yields a straight line with a slope of one. From the extrapolated intercept one derives a value of E_{CB} = -120 - 59pH [mV, vs. NHE]. As in the pH region investigates only few electrons leave the particle after excitation, band bending in the depletion layer region can be neglected and E_{CB} is practically identical with E_{fb}.

The position of the conduction band edge of the colloidal TiO₂ particle influences greatly the rate of the interfacial electron transfer. Figure 8 shows kinetic data obtained from the laser photolysis of solutions containing 500mg/1 TiO₂ and 10^{-3}M MV^{2+} at various pH values. The inserted oscillograms illustrate the temporal behavior of the MV^+ absorption at 602nm for pH 4 and 8, respectively. In both cases the 602 absorbance grows to a plateau according to a first order rate law. However, while at pH 4 this process requires several milliseconds to come to completion, only a few microseconds are needed at pH 8.
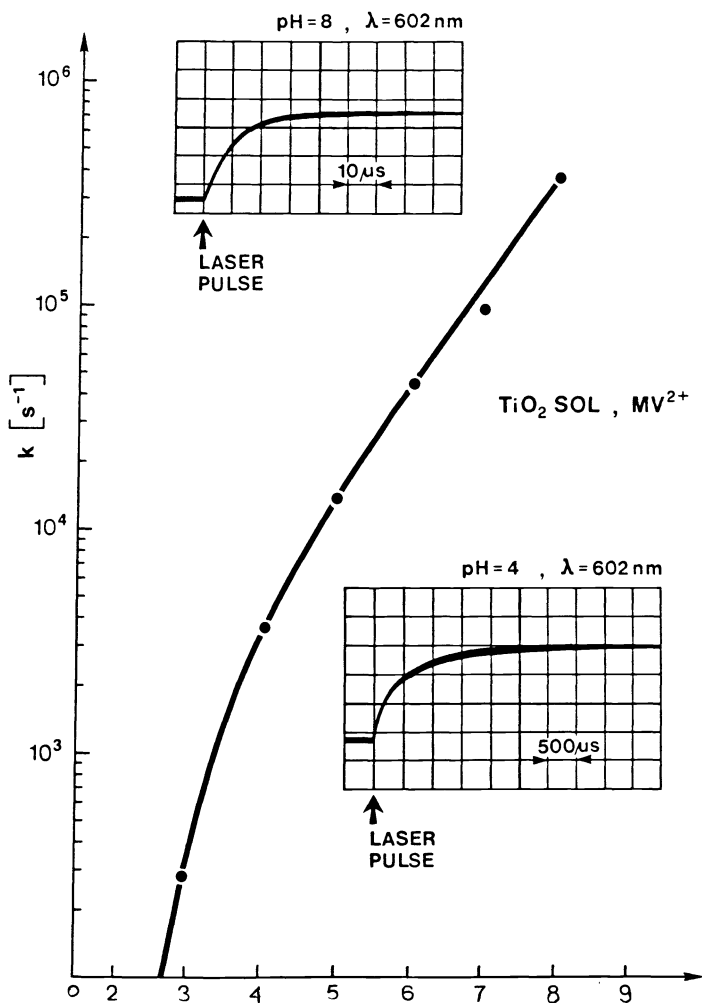
Fig. 8. Laser photolysis of TiO_2 colloids (500mg/l) at various pH values. Effect of pH on the rate constant of electron transfer from the conduction band to MV^{2+} $[MV^{2+}] = 10^{-3}M$. Insert: oscilloscope traces illustrating growth of MV^+ absorption at pH 8 and 4.

These phenomena may be rationalized in terms of the shift of the conduction band position of the TiO_2 particle with pH, affecting the match of electronic donor levels in the semiconductor (D_{el}^{occ}). The overlap integral of these two density of states functions determines the rate constant for heterogeneous electron transfer

$$k = v \int_0^\infty D_{el}^{occ} \cdot D_{el}^{unocc} \, dE \qquad (17)$$

where v is the tunneling collision frequency. D_{el}^{occ} is identical with the density of occupied electronic levels in the conduction band of the TiO_2 particle which peaks sharply at the conduction band edge E_{CB}. D_e^{unocc} is the distribution function for unoccupied levels in the $MV^{2+/+}$ redox system which has a maximum at $E^o(MV^{2+/+}) - \lambda$, where λ is the reorganization energy. At low pH the position of the TiO_2 conduction band is relatively positive and hence there is poor overlap of occupied states in the particle with unoccupied ones in the electrolyte. The situation improves with increasing pH where the conduction band position shifts to more negative values.

Using eq (12) one can quantitatively evaluate k_{et} as a function of pH from the measured bimolecular rate constants for MV^{2+} reduction. This evaluation (Ref. 20) shows that a Tafel relation is obeyed at pH > 5:

$$\log \frac{k_{et}}{k_{et}^o} = -(1 - \alpha) \frac{nF}{2.303 \ RT} \eta \tag{18}$$

where n is the number of electrons involved in the transfer step, F is Faradays' constant, k_{et}^o is the rate constant for electron transfer at the standard potential of the redox couple and α the transfer coefficient. At room temperature (T = 298°K) eq (18) assumes the form:

$$\log \frac{k_{et}}{k_{et}^o} = -\frac{(1 - \alpha)}{0.059} \eta \tag{19}$$

The overvoltage can be expressed in terms of the standard redox potential of the $MV^{2+/+}$ couple and the potential of the TiO_2 conduction band:

$$\eta = E_{CB}(TiO_2) - E^o(MV^{2+/+}) \tag{20}$$

Inserting the values for E_{CB} and $E^o(MV^{2+/+})$ in eq (20) gives:

$$\eta = 0.315 - 0.059 \ pH \tag{21}$$

and

$$\log \frac{k_{et}}{k_{et}^o} = (1 - \alpha) \ pH - (1 - \alpha) \ 5.34 \tag{22}$$

where 5.34 is the pH at which $\eta=0$. At this pH the specific rate of electron transfer $k_{et}^o = 4 \times 10^{-3} cm/s$ which corresponds to a moderate electrochemical rate constant. From the slope of the Tafel line one obtains $\alpha=0.52$ for the transfer coefficient which indicates a symmetrical transition state.

This analysis provides new physical insight into the phenomenon associated with light-activated charge transfer across the semiconductor solution interface. The kinetic equations derived allow the determination of important electrokinetic parameters, such as the heterogeneous rate constant for electron transfer and the transfer coefficient. In the case of MV^{2+} reduction by conduction band electrons from TiO_2 particles, the interfacial electron transfer step is rate controlling at lower pH when the over voltage available to drive the reaction is small. At higher pH mass transfer effects become increasingly important and determine the overall reaction rate.

Dynamics of hole transfer from colloidal TiO_2 to reductants in solution
Using similar laser photolysis technique the reaction of valence band holes in colloidal TiO_2 particles (h^+) with electron donors, such as halide ions or SCN^-, has also been investigated. (Ref. 21) The oxidation of these species follows the eq

$$X^- \xrightarrow{h^+} X\cdot \xrightarrow{+X^-} X_2^- \tag{23}$$

and thus results in the formation of halide or $(SCN)_2^-$ radical anions. These species can be readily analyzed by their caracteristic absorption spectrum. Using fast optical analysis we found that reaction (23) occurs extremely rapidly and is completed already within the ∿10ns laser pulse. The hole transfer was shown to involve only species adsorbed to the surface of the colloidal TiO_2 particle. The efficiency of the process follows the sequence $Cl^- < Br < SCN^- \sim I^-$ and hence is closely related to the redox potential of the X^-/X_2^- couple. Further studies showed that the yield of X_2^- decreases strongly with increasing pH and this effect has been attributed to the competition of water oxidation with reaction (23).

Interfacial charge transfer in colloidal CdS solutions
Cadmium sulfide has been extensively investigated as an electrode material in photoelectrochemical cells. (Ref. 22) Studies on suspensions of CdS powders, on the other hand, have been comparatively scarce, (Ref. 23) but have gained considerable momentum since light-induced H_2 (Ref. 24) and co-generation of H_2 and O_2 (Ref. 25) was found to occur on noble metal loaded CdS particles. Water and H_2S cleavage can also be achieved with CdS sols and for this reason we shall briefly discuss some laser studies with colloidal solutions of this material.

The UV-visible absorption spectrum of the CdS sol, prepared by precipitation from a $Na_2S/Cd(NO_{3/2})$ solution in the presence of hexametaposphate as stabilizing agent, is distinguished by a sharp band edge rising steeply towards the blue below 520nm. The onset coincides exactly with the band gap of crystalline CdS electrodes, i.e. 2.4eV. Electron diffraction studies showed that the colloidal particle (hydrodynamic radius ca. 150Å) is a single crystal

of Wurtzit structure. Excitation of the CdS sol leads to luminescence which is distinguished by a broad maximum around 700nm. Addition of solutes such as MV^{2+} to the solution shifts the maximum to 520nm. Using single photon counting technique, we determined the lifetime of the luminescence as $\tau = (0.3\pm0.2)$ns. (Ref. 19)

From the short lifetime of an electron-hole pair in colloidal CdS one would infer that e^-_{CB} could only reduce species adsorbed to the surface of the particle. Diffusional displacement required for reaction with acceptors in the bulk would be too slow to be able to compete with $e^-_{CB}\ldots h^+$ annihilation. This idea is fully borne out by experimental results. Thus, in the presence of MV^{2+} as acceptor the blue color of MV^+ appears promptly and within the laser and no slow growth of the 602nm absorption is observed as was the case for TiO_2. In the absence of O_2 the signal of MV^+ remains stable. An intense blue color is developed under continous exposure to visible light in agreement with the observations made by Harbour and Hair on macrodisperse CdS powders. (Ref. 23a)

The yield of MV^+ obtained by flash irradiation of the CdS sol with 487nm laser light was found to increase with MV^{2+} concentration increasing the latter from 0.2 to 5×10^{-3}M results in an augmentation of (MV^+) from 0.3 to 2×10^{-5}M. Apparently at the higher MV^{2+} concentration the coverage of the CdS particle surface with MV^{2+} is increased. This enhances the rate of interfacial electron transfer which can compete more efficiently with electron-hole recombination.

An interesting application of the laser technique is the study of electron and hole reaction with catalysts deposited on the surface of the semiconductor particle. Thus, in the case of the MV^{2+} reduction by CdS conduction band electrons the yield of MV^+ is reduced if the particles are loaded with Pt. This is due to the trapping of e^-_{CB} by Pt-sites on the surface which occurs in competition with MV^{2+} reduction.

$$e^-_{CB} + MV^{2+} \xrightarrow{\ \ k(MV^{2+})\ \ } MV^+ \tag{24}$$

$$e^-_{CB} + Pt \xrightarrow{\ \ k(Pt)\ \ } Pt^- \xrightarrow{\ -H_2O\ } \tfrac{1}{2}H_2 + OH^- \tag{25}$$
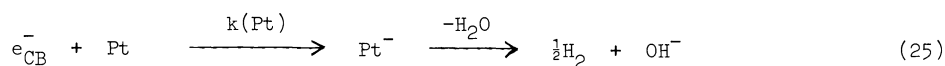
Electrons undergoing reaction (25) can no more contribute to the yield of MV^+ as they are used to generate hydrogen from water under the prevailing pH conditions. This technique is potentially useful in that it allows for rapid screening and optimization of hydrogen evolving colloidal semiconductor systems. (Ref. 25).

VISIBLE LIGHT INDUCED WATER CLEAVAGE THROUGH DIRECT BAND GAP EXCITATION OF COLLOIDAL SEMICONDUCTORS

In this section we shall describe a water photolysis system based on band gap excitation of semiconductor dispersions. This provides an illustrative example for the application of the concepts derived in the preceeding chapters to develop photolytic, fuel producing systems. A semiconductor particle is charged with both a catalyst for water oxidation (RuO_2) and reduction (Pt). Band gap excitation produces an electron/hole pair in the particle. Both charge carriers diffuse to the interface where hydrogen and oxygen generation occurs, Fig. 9.
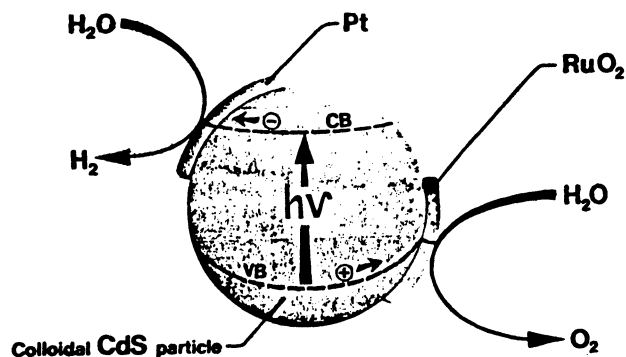
Fig. 9. Schematic illustration of a water cleavage process mediated by a CdS particle.

TiO$_2$ was the first material to be employed in such a system. The domain of photoactivity has recently been displaced in the visible by using n-CdS particles as carriers for Pt and RuO$_2$. An undesirable property of this material is that it undergoes photocorrosion under illumination. Holes produced in the valence band migrate to the surface where photocorrosion occurs, i.e.

$$CdS \; + \; 2h^+ \; \longrightarrow \; Cd^{2+} \; + \; S \qquad\qquad (26)$$
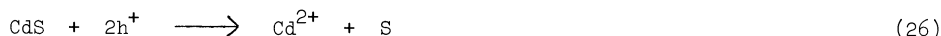
We observed recently (Ref. 26) that loading of CdS particles with an ultrafine deposit of RuO$_2$ prevents photodecomposition through promotion of water oxidation according to

$$4h^+(CdS) \; + \; 2H_2O \; \xrightarrow{\;(RuO_2)\;} \; O_2 \; + \; 4H^+ \qquad\qquad (27)$$
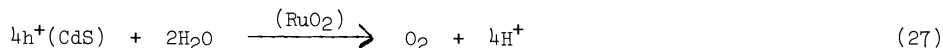
Sustained water cleavage by visible light is observed when CdS particle loaded simultaneously with Pt and RuO$_2$ are used as photocatalyst. Hydrogen and oxygen are generated by conduction band electrons and valence band holes, respectively, produced by band gap excitation. This water cleavage phenomena can be illustrated unambiguously by gas chromatography analysis. Figure 10 shows results obtained from visible light ($\lambda > 420$nm) irradiation of 25ml aqueous solution (pH 13) containing 25mg CdS loaded with 3mg RuO$_2$ (deposition of RuO$_2$ was carried out via thermal decomposition of (Ru)$_{13}$(CO)$_{12}$ in Ar at 300°C for 30 min.). Initially there are only traces of H$_2$ generated since the reduction of H$_2$ Pt Cl$_6$ occurs in preference over H$_2$O reduction. However, the peaks of H$_2$ and O$_2$ grow concommittantly after this induction period. Note that the ratio of the N$_2$ to O$_2$ peak heights decreases with irradiation time indicating that the oxygen signal does not arise from air contamination. Under stationary conditions such a system delivers ca 50μl/h of H$_2$ and 25μl/h of O$_2$ (p=1 atm, room temperature) corresponding to a quantum yield of H$_2$O cleavage of ca 0.2%.

VISIBLE LIGHT INDUCED WATER
CLEAVAGE IN CdS DISPERSIONS
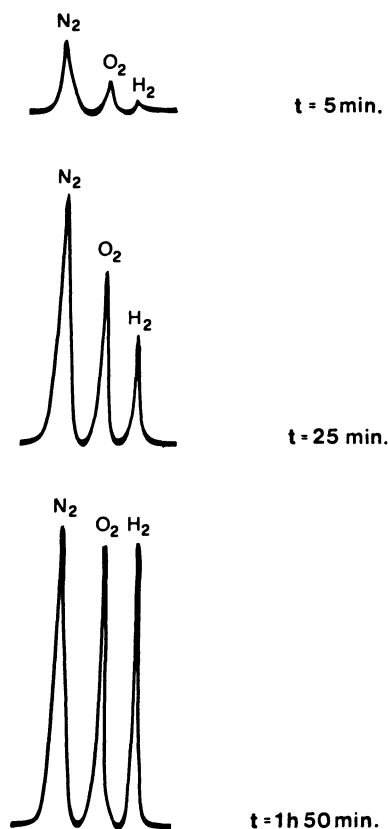
Fig. 10. Gaschromatographic evidence for the formation of hydrogen and oxygen by visible light irradiation of CdS particles loaded with RuO$_2$
[CdS] = 1g/1   [RuO$_2$] = 150mg/1   [Li$_2$CO$_3$] = 0.1M   pH = 13

Apart from water, other agents such as hydrogen sulfide have the potential to play an important role as an alternative source for hydrogen production from sunlight. Sulfides occur widely in nature and H_2S is produced in large quantities as an undesirable by-product in coal and petrol related industries. Therefore, catalytic systems in which the process

$$H_2S \xrightarrow{h\nu} H_2 + S \tag{28}$$

is driven by visible light should be of significant interest. As the standard enthalpy of reaction (1) is +9.4 kcal/mol this provides a method for energy conversion and storage as well as for recycling of H_2 employed in hydrodesulfurization processes.

When RuO_2 loaded CdS particles are dispersed in aqueous sulfide solutions and illuminated with visible light, hydrogen is generated at an astonishingly high rate. Results obtained from irradiating a 25ml solution containing 25mg CdS loaded with 0.025mg RuO_2 in the presence of 0.1M Na_2S (pH 3) showed that after a brief induction period the H_2 generation rate established itself at 3.2ml/h until almost all the H_2S has been consumed.

A detailed investigation established that the efficiency of hydrogen generation depends on both solution pH and RuO_2 loading. At pH 13 and 0.5% RuO_2 loading of the CdS particles the rate of H_2 generation is 10ml/h corresponding to a quantum yield of 35%.

These observations may be rationalized in terms of band gap excitation of the CdS particles producing electrons in the conduction and holes in the valence band. (Ref. 27) The former migrate to the interface where reduction of water to hydrogen occurs

$$2\,e_{cb}^- + 2H^+ \longrightarrow H_2 \tag{29}$$

while the holes react with H_2S (or HS^- depending on pH) under sulphur formation

$$H_2S + 2h^+ \longrightarrow 2H^+ + S \tag{30}$$

The overall reaction corresponds to splitting of H_2S into hydrogen and sulphur by four quanta of visible light.

Sulphur formed concomitantly with H_2 in the photoreaction does not seem to interfer with water reduction. It appears therefore that the reduction of sulphur by conduction band electrons of CdS, though thermodynamically favored, is strongly inhibited for kinetic reasons. This explains why the H_2S photocleavage can proceed almost to completion without decrease in the reaction rate.

Oxygen, on the other hand, can compete with water reduction by conduction band electrons. Thus, at pH 13 and 0.3% loading of CdS with RuO_2, rH_2 is decreased from 9ml/h to 8ml/h when air saturated instead of deaerated suspensions are illuminated. Still, this competition of oxygen is surprisingly ineffecient.

Apart from its importance in solar energy research and for the treatment of H_2S containing waste streams, the H_2S cleavage reaction mimics also in an intriguing fashion the function of photosynthetic bacteria which frequently use sulfides as electron donors for the reduction of water to hydrogen.

CONCLUSIONS

Molecular assemblies such as micelles, colloidal semiconductors and ultrafine redox catalysts provide suitable microscopic organization to accomplish the difficult task of light energy harvesting and subsequent fuel generation. New kinetic models had to be conceived to provide basis for the understanding of the dynamics of energy and electron transfer processes in these aggregates. In this review a first attempt was made to outline and summarize the basic features of these processes and to illustrate the general applicability of the kinetic concepts to different types of colloidal assemblies. Research activity in this field is increasing rapidly and many exciting new discoveries have been made during the last years. As for the application of these systems in light induced water cleavage devices, work in the future will be directed to improve the efficiency of such devices by identifying new photocatalysis and solving the problem of hydrogen/oxygen separation. Colloidal semi-

conductors will certainly play a primordial role in this development. Together with other functional organizations they have the key advantage that light-induced charge separation and catalytic events leading to fuel production can be coupled without intervention of bulk diffusion. Thus a single colloidal semiconductor particle can be treated with appropriate catalysts so that different regions function as anodes and cathodes. It appears that this wireless photoelectrolysis could be the simplest means of large scale solar energy harnessing and conversion.

REFERENCES

1. a) D.O. Hall, Fuel 57, 322 (1978);
   b) P. Cuendet and M. Grätzel, Experientia 38, 223 (1982), and reference cited therein.
2. a) M. Calvin, Photochem. Photobiol. 23, 425 (1976);
   b) J.J. Katz and M.R. Wasielewski, in: Biotechnology and Bioengineering Symposium No. 8
      Ed. C.D. Scott. Interscience, New York 1979.
3. S.A. Alkaitis, G. Beck and M. Grätzel, J.Am.Chem.Soc. 97, 5723 (1975).
4. P.P. Infelta, M. Grätzel and J.K. Thomas, J. Phys. Chem. 78, 190 (1974).
5. M. Maestri, P.P. Infelta and M. Grätzel, J. Chem. Phys. 69, 1522 (1978).
6. K. Kalyanasundaram and M. Grätzel, Helv. Chim. Acta 63, 478 (1980).
7. C.K. Grätzel and M. Grätzel, J. Phys. Chem., in press.
8. B. Razem, M. Wong and J.K. Thomas, J.Am.Chem.Soc. 100, 1679 (1978).
9. Y. Waka, K. Hamamoto and N. Mataga, Chem. Phys. Lett. 53, 242 (1978).
10. C. Wolff and M. Grätzel, Chem. Phys. Lett. 52, 542 (1977).
11. Y. Moroi, A. Braun and M. Grätzel, J.Am.Chem.Soc. 101, 567 (1979).
    Y. Moroi, P.P. Infelta and M. Grätzel, J.Am.Chem.Soc. 101, 573 (1979).
12) M.D. Hatley, J.J. Kozak, G. Rothenberger, P.P. Infelta and M. Grätzel,
    J. Phys. Chem. 84, 1508 (1980).
13. a) R. Humphry-Baker, Y. Moroi, M. Grätzel, P. Tundo and E. Pelizzetti,
       Angew. Chem. Int. Ed. 18, 630 (1979);
    b) R. Humphry-Baker, Y. Moroi, M. Grätzel, P. Tundo and E. Pelizzetti,
       J.Am.Chem.Soc. 102, 3689 (1980);
    c) K. Monserrat, M. Grätzel and P. Tundo, J.Am.Chem.Soc. 102, 3689 (1980);
    d) Y. Moroi, E. Pramauro, M. Grätzel, E. Pelizzetti and P. Tundo,
       J. Coll. Int. Sci. 69, 341 (1979);
    e) J. Le Moigne, P. Gramein and J. Simon, J. Coll. Int. Sci. 60, 565 (1977).
14. R. Humphry-Baker, A.M. Braun and M. Grätzel, Helv. Chim. Acta 64, 2036 (1981).
15. M.-P. Pileni, A.M. Braun and M. Grätzel, Photochem. Photobiol. 31, 423 (1980).
    P.-A. Brugger and M. Grätzel, J.Am.Chem.Soc. 102, 2461 (1980).
    P.-A. Brugger, P.P. Infelta, A.M. Braun and M. Grätzel, J.Am.Chem.Soc. 103, 320 (1981).
16. a) M. Grätzel, Isr. J. Chem. 18, 364 (1979).
    b) M. Grätzel, Ber. Bunsenges. Phys. Chem. 84, 981 (1980).
    c) M. Grätzel, Acc. Chem. Res. 14, 376 (1981).
17. F. Williams and A.J. Nozik, Nature 271, 137 (1979).
18. W.J. Albery and P.N. Bartlett have solved the reaction-diffusion equation for a similar
    case, where a relay compound transfers electrons to a colloidal Pt particle, c.f.
    Disc. Faraday Soc. 70, 421 (1980).
19. a) D. Duonghong, E. Borgarello and M. Grätzel, J.Am.Chem.Soc. 103, 4685 (1981);
    b) D. Duonghong, J. Ramsden and M. Grätzel, J.Am.Chem.Soc. 104, 0000 (1982).
20. M. Grätzel and A.J. Frank, J. Phys. Chem. 86, 0000 (1982).
21. J. Moser and M. Grätzel, Helv. Chim. Acta 65, 0000 (1982).
22. G. Hodes, D. Cahen, J. Manassen and M. David, J. Electrochem. Soc. 127, 2252 (1980).
23. a) F.D. Saeva, G.R. Olin and J.R. Harbour, J.Chem.Soc. Chem.Commun. 401 (1980);
    b) J.R. Harbour and M.L. Hair, J. Phys. Chem. 81, 1741 (1977).
    c) S.N. Frank and A.J. Bard, J. Phys. Chem. 81, 1484 (1977).
24. J.R. Darwent and G. Porter, J.Chem.Soc. Chem.Commun., 145 (1981).
25. K. Kalyanasundaram, E. Borgarello, D. Duonghong and M. Grätzel, Angew. Chem. 93, 1012
    (1981).
26. K. Kalyanasundaram, E. Borgarello and M. Grätzel, Helv. Chim. Acta 64, 362 (1981).
27. E. Borgarello, K. Kalyanasundaram, M. Grätzel and E. Pelizzetti,
    Helv. Chim. Acta 65, 243 (1982).